Selective injection of magnetic domain walls in Permalloy nanostripes

Johanna Akerman, Manuel Muñoz, Marco Maicas, and José L. Prieto

Citation: Journal of Applied Physics **115**, 183909 (2014); doi: 10.1063/1.4876302
View online: http://dx.doi.org/10.1063/1.4876302
View Table of Contents: http://scitation.aip.org/content/aip/journal/jap/115/18?ver=pdfcov
Published by the AIP Publishing

JOURNAL OF APPLIED PHYSICS **115**, 183909 (2014)

Selective injection of magnetic domain walls in Permalloy nanostripes

Johanna Akerman,[1] Manuel Muñoz,[2] Marco Maicas,[1] and José L. Prieto[1]
[1]*Instituto de Sistemas Optoelectrónicos y Microtecnología (ISOM), Universidad Politécnica de Madrid, Avda. Complutense s/n, E-28040 Madrid, Spain*
[2]*IMM-Instituto de Microelectrónica de Madrid (CNM-CSIC), Isaac Newton 8, PTM, Tres Cantos, E-28760 Madrid, Spain*

(Received 18 March 2014; accepted 1 May 2014; published online 14 May 2014)

This work explores the conditions that allow the injection and pinning of different magnetic domain walls (DWs) in Permalloy nanostripes with notches of different shapes. The injection is done under a constant external field by applying a 10 ns current pulse through an adjacent current line. The type of DW is identified by its anisotropic magnetoresistance (AMR). We find that, while a quasi-static pinning (nucleating at zero field and propagating the DW to the notch by slowly increasing the external field) would allow to distinguish different types of DWs pinned at the notch, a dynamic pinning (nucleating, propagating, and pinning the DW under a constant non-zero magnetic field) makes the discrimination of different DWs very difficult. Micromagnetic simulations indicate that the AMR of the different types of DWs become quite similar to each other as the injection field increases. This might explain why at large injection fields, usually only one or two values of resistance are detected, depending on the shape of the notch. Therefore, caution should be taken when establishing a one-to-one relationship between a type of DW and a value of resistance, especially if the injection is done under a non-zero external magnetic field. © *2014 AIP Publishing LLC*. [http://dx.doi.org/10.1063/1.4876302]

I. INTRODUCTION

The access to nanofabrication techniques has boosted the number of applications based on magnetic domain walls (DWs) like magnetic logic,[1] memory devices,[2] or RF oscillators.[3] The functionality in all these applications is based on the exquisite control of the DW dynamics in magnetic nanostripes. This exquisite control could be achieved by reliably injecting the DW in the stripe, by controlling the pinning process in an engineered defect, and by obtaining a defined depinning process, i.e., always at the same value of applied current or external magnetic field. These three aspects (injection, pinning, and depinning) have been intensively studied in recent years, especially in Permalloy (Py) nanostripes. Despite this large effort, the overall picture of the behavior of magnetic domain walls in Py nanostripes is not perfectly clear. For instance, although the pinning and depinning processes of the different DWs in a triangular notch patterned on a Py nanostripe (300 nm wide and 10 nm thick) were pretty much completely characterized by the group of Parkin at IBM[4,5] and others,[6] the types of DWs pinned, their chirality or their characteristic depinning current or field, may change if the notch has slightly different dimensions,[7,8] the stripe has different thickness,[9] or even if the DW is pinned by a different procedure.[10] Additionally, there is a stochastic component in both the injection of the DW[11] and in its pinning-depinning process[12,13] which may be partly intrinsic to the nature of the travelling DW at a non-zero temperature[14] and partly due to the unavoidable defects introduced during the nano-fabrication process.

Therefore, it is still quite difficult to know which type of DW will likely pin in a ferromagnetic nanostripe with a patterned notch of a given shape. While giving a precise answer to this question is perhaps impossible, it is important to know the conditions that favor the pinning of a particular type of DW. For instance, in studies of current induced depinning, the exact influence of Joule heating[15–17] or spin torque transfer, requires a good knowledge of the spatial distribution of current and magnetization around the notch, so an experiment could be properly compared to the micromagnetic simulations. Ideally then, the type and structure of the DW depinned in every experiment should be known.

In this work, we explore the conditions for DW injection that allow a selective pinning of the different types of DWs in Permalloy nanostripes. The study is done for notches of three different shapes in nanostripes 300 nm wide and 10 nm thick, where transversal and vortex walls of both chiralities are energetically viable for certain injection conditions.

When the DW is nucleated, propagated, and pinned under a fixed non-zero external magnetic field, we find that discriminating the chirality of the pinned DWs by their value of anisotropic magnetoresistance (AMR) is possible for many injection fields. We also find an unjustified apparent absence of some types of DWs when the injection is done at high or even moderated external fields. Micromagnetic simulations indicate that the AMR of the different types of DW becomes quite similar to each other as the injection field increases. This could explain why, when the injection is done at a large field, we only find one or two AMR values in the histograms, depending on the shape of the notch.

II. EXPERIMENTAL DETAILS

The experimental set up is pictured in Fig. 1. The nanostripes are deposited by DC sputtering on a Si/SiO_2 substrate with a structure Ta(2 nm)/Py(10 nm)/Ta(2 nm)/Pt(2 nm) and patterned by lift-off in the dimensions mentioned above. The contacts are 500 nm wide, patterned also by lift-off with the

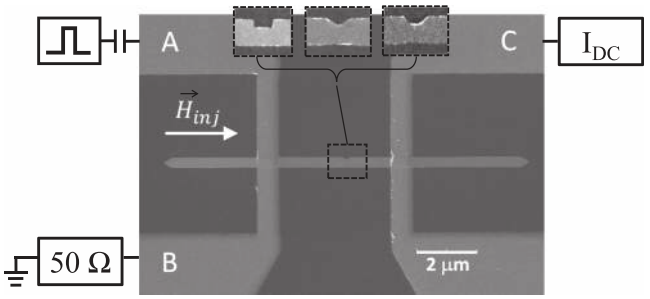

FIG. 1. Experimental set-up with a 300 nm wide Permalloy nano-stripe with a notch in the middle. Three different shapes of the notch have been studied: square, triangular, and circular.

structure Cr(5 nm)/Au(50 nm). The study is done on a single chip were all the stripes should be structurally identical, except for the shape of an engineered notch between the contacts, 300 nm wide and 100 nm deep (see Fig. 1). In some of the devices, though, unwanted structural defects made the results largely stochastic. Therefore, only results that could be contrasted in different stripes are presented here.

The DW is injected as follows: the stripe is saturated in the negative direction, then a positive field H_{inj} is applied, and once this positive field is stable, a 10 ns, 1.4 V ($3{\cdot}10^7$ A/cm^2) current pulse is sent from pad A to pad B in Fig. 1. This method of injecting the DW in ferromagnetic nanostripes is fast and very reliable,[11,18,19] which is very useful for studies where statistics are important to evaluate stochastic effects. The presence and the type of DW injected in the nanostripe is detected by measuring the drop in the resistance of the wire due to the AMR introduced by the DW. This is done using a lock-in technique compensating the resistance of the stripe with a calibrated external resistance.[13] The measuring current is 100 μA ($2{\cdot}10^6$ A/cm^2) at 82 Hz, which is small enough to be neglected in terms of spin transfer torque effects and it is effectively constant during the few nanoseconds that the injection and the pinning process take.

In order to help with the interpretation of the experimental results, we have performed micromagnetic simulations using OOMMF software package (release 1.2a4). Standard Py parameters were considered: saturation magnetization $Ms = 8.6{\cdot}10^5$ A/m, exchange constant, $A = 13{\cdot}10^{-12}$ J/m, and damping $\alpha = 0.01$. A strong perpendicular to plane magnetic field introduced by the injection current pulse (5.5 mT)[18] was included in the simulations. In order to estimate the AMR of each type of DW, the current was always assumed along the length of the stripe, which is not the case in the notch. Therefore, although the simulations provide good comparative AMR values for the different types of DW within the same type of notch, they are only indicative if they are compared between the different notches.

Fig. 2(a) shows a sequence of pinning and depinning of a Transversal DW (clockwise) in a stripe with a square notch. The AMR of the DW is calculated for the different fields and it is also displayed in Fig. 2(a). The resistance decreases from a free DW (2 mT) to a pinned DW (3 mT). When the field increases to 4 mT, the DW has crossed the notch and it is effectively depinned. For larger fields, a long tail of the DW remains attached to the notch, although this is

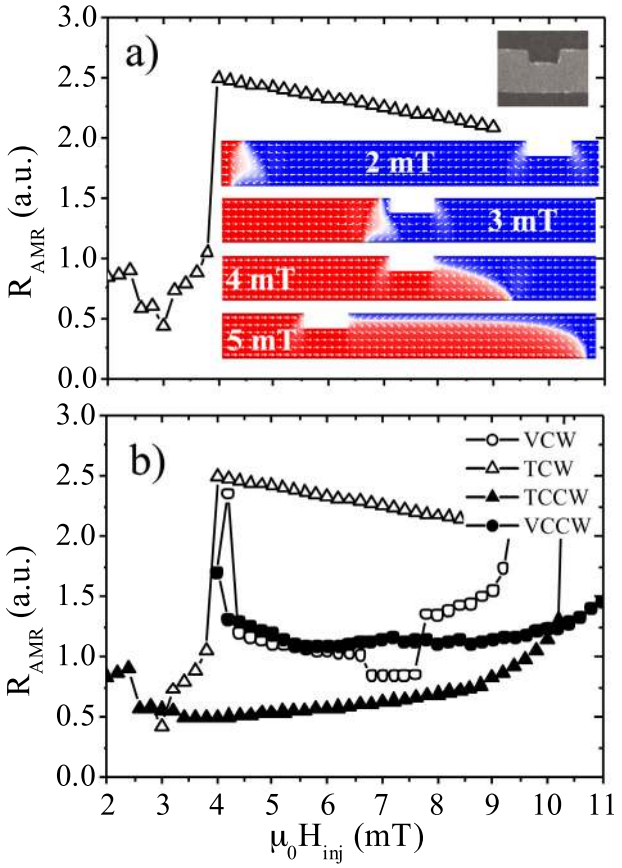

FIG. 2. (a) Sequence of the pinning and depinning of a transversal clockwise DW in a square notch. The AMR of the DW is extracted for each field. (b) AMR of the different types of DW during their sequence of pinning-depinning in a square notch: Transversal Clockwise (TCW) and Counterclockwise (TCCW), and Vortex Clockwise (VCW) and Counterclockwise (VCCW).

unlikely going to happen in experiments due to thermal activation. The magnetic fields required for the depinning of the DW in the micromagnetic simulations are larger than the ones observed in the experiments by approximately a factor of 5. This is usually the case due to the lack of thermal activation in the simulations.[9]

The plot of Fig. 2(a) is obtained for each type of DW and the results are shown in Fig. 2(b). This simulation was repeated for every shape of notch under study. The results will be discussed and critically compared to the experimental findings in Subsections III A and III B. In Fig. 2(b), it is important to highlight the fact that the AMR of the different DWs changes significantly as the injection field increases and the structure of the DW accommodates to the notch before depinning. This makes the AMR of the DWs dependent on the injection process. For instance, if a clockwise vortex DW (VCW) is injected at $H_{inj} = 0$ and then driven to the notch by a small external field just above the propagation field of the stripe, the DW is likely going to hold its structure and it gets pinned on the arriving edge of the notch. This VCW would have the AMR value corresponding to 4.2 mT in Fig. 2(b), which is larger than the AMR of any transversal DW. On the other hand, if the VCW is injected under a $H_{inj} = 7$ mT, the vortex will get pinned inside the notch and its distorted structure would result on a considerably smaller AMR value. Incidentally, this smaller AMR value would be

quite similar, for instance, to the value for a clockwise transversal DW pinned at 3.5 mT. This point will be quite relevant later, when we discuss the experimental results.

III. EXPERIMENTAL RESULTS

A. Identifying the different magnetic domain walls

First, we measured the propagation field in our wires. The DW is injected at $H_{inj} = 0$, and then the external field is increased very slowly towards negative or positive values until the DW disappears or changes slightly its resistance (i.e., it is pinned at the notch). The propagation field was found to be very small (~2 Oe), which indicates the good quality of the fabrication method and the small amount of random pinning defects.

Next, we want to confirm that the DW changes its characteristic AMR when it arrives to the notch, as predicted by the micromagnetic simulations (Fig. 2). We inject the DW without any external magnetic field ($H_{inj} = 0$) and measure its resistance. Note that, due to the strong perpendicular to plane magnetic field induced by the injection pulse, for Py stripes of these dimensions, only transversal DWs are injected if $H_{inj} = 0$.[18,20] Once the DW is nucleated, the external magnetic field is increased slowly to a given value and the DW resistance is measured again. We repeat this process 400 times in order to build a histogram with proper statistics. Bearing in mind the small propagation field, it is safe to assume that the DW will arrive to the notch once the external field is higher than the propagation field (2 Oe).

Fig. 3 shows the results for a square and a triangular notch. In the case of a stripe with a square notch (Fig. 3(a)) for $H_{inj} = 0$, the peak is centered on 0.2 Ω which should be the resistance of a free transversal DW.[20] There is no peak centered on 0 Ω for $H_{inj} = 0$, meaning that the 400 events injected a DW successfully. When the field is increased slowly to 10 Oe after injection, the histogram splits into two peaks and a hump in the middle, indicating three different types of DW pinned at the notch. If the field is increased to 35 Oe after the injection at 0 Oe, the peak with higher resistance disappears, the peak at 0.19 Ω gets smaller and the peak at 0.23 Ω (the hump at 10 Oe) gets larger. Finally, increasing the field to 40 Oe after injection, only the smaller peak at 0.19 Ω remains and most of the events have gone to 0 Ω,

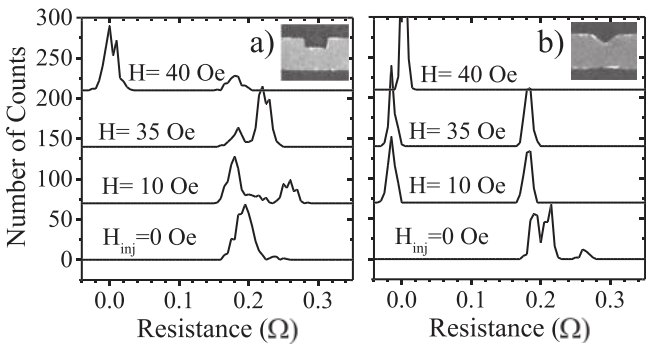

FIG. 3. Histograms with the resistance of the injected DWs at $H_{inj} = 0$ (the DW is not pinned at the notch) and the subsequent histograms when the external magnetic field is slowly increased to a set value H after injection. Measurements for a square notch in (a) and for a triangular notch in (b).

meaning that most of the DWs have been depinned by the external field. In the simulations, the smaller AMR corresponds to the transversal counterclockwise (TCCW), which is one of the DW with larger depinning field. Therefore, we can safely assume that 0.19 Ω corresponds to TCCW pinned at the arriving edge of the notch (the left edge in Fig. 1).

For a triangular notch (Fig. 3(b)), the injection at $H_{inj} = 0$ produces a double peak centered on 0.2 Ω. When the field increases, most of the DWs get depinned and only events of 0.19 Ω remain. The different resistance peaks present in Fig. 3 have been associated previously with different types of DWs[5,19]: 0.19 Ω for TCCW, 0.23 Ω for transversal clockwise (TCW), and 0.27 Ω for vortex counterclockwise (VCCW). Occasionally, in some devices we have found a fourth value of 0.32 Ω, which might be associated to VCW.

B. Different injection conditions

In the following measurements, the DW is nucleated and driven to the notch at a certain H_{inj}. Only for $H_{inj} = 0$ or smaller than the propagation field (~2 Oe), the DW is not assumed pinned at the notch. It is important to remember that for an injection pulse of 1.4 V and in Py stripes of these dimensions, only transversal DWs are injected if $H_{inj} = 0$.[18,20] For larger amplitude of the injection pulse, the chances of nucleating vortex DWs increase but equally the chances of having metastable states of the pinned DWs also increase, making the identification of the type of DW more difficult. Therefore, although we have studied the pinning-depinning process at different injection voltages, here we present only the more repeatable results at 1.4 V.

We begin by analyzing the pinning conditions in stripes with a triangular notch. Figure 4 shows the results for selected injection fields in a stripe with a triangular notch. As expected, for $H_{inj} = 0$, there is only one peak centered on 0.2 Ω, corresponding to a free (not pinned) transversal DWs. When $H_{inj} = 10$ Oe, which is roughly the value of the Walker breakdown in these stripes,[4,21] the DW undergoes periodic transformations from transversal to vortex as it travels towards the notch. Therefore, any type of DW could potentially be pinned in the notch. This is indeed what we find and four peaks, corresponding in principle to the four types of DWs, are present in the histogram at $H_{inj} = 10$ Oe. Nevertheless, throughout the devices measured, many times the peaks for the vortex walls (the two with highest resistance) are almost negligible. Finally, for $H_{inj} = 20$ Oe, only the peaks at 0.19 Ω and 0.23 Ω remain. As it was mentioned in the introduction, the conditions of pinning and depinning in a triangular notch in Py nanostripes, have been previously characterized, mainly by the group of Parkin at IBM,[4,5] but also by other groups.[6,9,10] Our experimental results for a triangular notch confirm previous observations.

The micromagnetic simulations (Fig. 4(b)) agree to a large extent with the experiments. Both transversal DWs have the same resistance before they are pinned. Once they are pinned, the TCW increases the resistance while the TCCW decreases its resistance, in agreement with the experimental results. On the other hand, Fig. 4(b) and other works,[9,19,22] show that both vortex get depinned at a larger

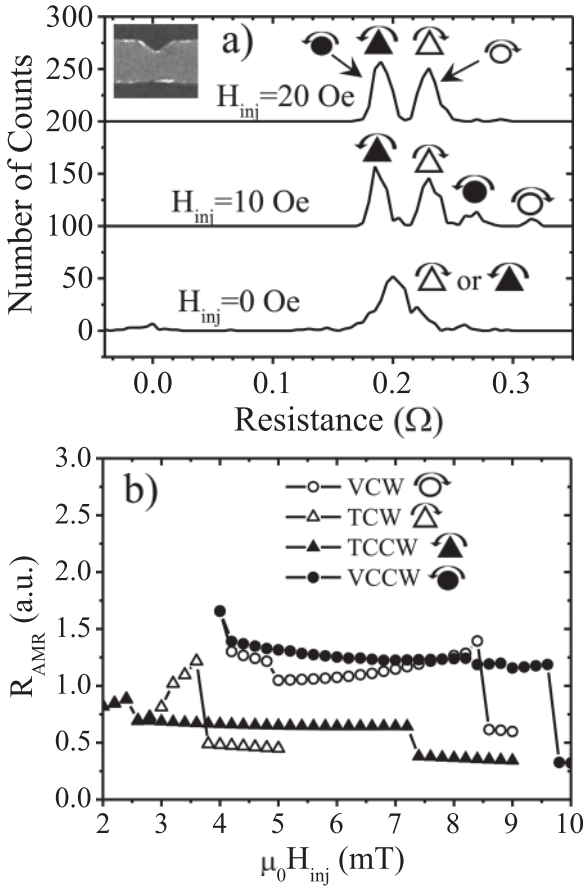

FIG. 4. (a) Histograms for different injection fields H_{inj} in a stripe with a triangular notch. The peaks are labeled with a small cartoon representing the type of DW as shown by the symbols in (b). (b) AMR obtained from the micromagnetic simulations, for each type of DW for different stages of the pinning-depinning process.

field than any of the transversal DWs. Therefore, the absence of the vortex peaks at $H_{inj} = 20$ Oe in Fig. 4(a), requires an additional explanation.

First, the simulations show a transformation from VCCW to TCCW before depinning (not shown here but also previously observed by other authors[9,19,22]). This transformation might justify the absence of the VCCW peak in the histogram at $H_{inj} = 20$ Oe, as this vortex DW might contribute to the 0.19 Ω peak of the TCCW. On the other hand, VCW does not transform to a TCW but VCW must be travelling through the wire at $H_{inj} = 20$ Oe because there are no depinning events (no counts at 0 Ω). The peak for VCW (0.32 Ω) is only found occasionally around 10 Oe. Therefore, we have to assume that the AMR of the VCW becomes quite similar to 0.23 Ω when this DW is pinned at large fields. In fact, the simulations point out in this direction. In Fig. 4(b), we can see for instance that a VCW pinned between 4.5 and 8 mT could show a very similar AMR to a TCW pinned in the notch (pinned at 3.5 mT). Therefore, the histograms of DWs pinned in a triangular notch when injected at high fields, typically showing two peaks at 0.19 Ω and 0.23 Ω, seem to include TCCW plus VCCW transformed to TCCW (0.19 Ω peak) and TCW plus VCW (0.23 Ω peak). Note also that the peaks in the histogram at $H_{inj} = 20$ Oe are slightly broader than the ones at $H_{inj} = 10$ Oe, possibly because they are accommodating more microstates of the pinned DWs.

In order to explore if the vortex DWs can be discriminated in a current induced injection process, we repeated the same experiment for a nano-stripe with a square notch.

Fig. 5 shows the histograms for the three selected injection fields 0, 10, and 20 Oe. For $H_{inj} = 0$ Oe, only the peak for not-pinned transversal DW shows. For $H_{inj} = 10$ Oe, the peak splits in two with the values for both transversal DWs. Finally, for $H_{inj} = 20$ Oe, only one broad peak centered on 0.23 Ω remains, while there are still no depinning events at this field. There is no sign of vortex DWs in the histograms (0.27 Ω and 0.32 Ω). As all the stripes are identical except for the shape of the notch, we should assume that all the types of DW are present in the stripe for $H_{inj} = 10$ Oe or higher, like in the case of stripes with a triangular notch.

The micromagnetic simulations for a square notch (Fig. 2(b)) show again only a transformation from VCCW to TCCW, although not as "clean" as in the case of a triangular notch. For the square notch, as the field increases, the core of the VCCW is pushed upwards towards the left corner of the notch and it stays there while a 360° transversal structure forms within the notch. Therefore, the lack of vortex peaks at any field and the single peak centered on 0.23 Ω for $H_{inj} = 20$ Oe can only be explained if the AMR values for the different DWs become quite similar to each other. By looking at Fig. 2(b), we see that the AMR for both vortex DW pinned at the notch (4–7 mT) is quite similar to the AMR of a pinned TCW (3.5 mT). This might justify the presence of only two peaks at $H_{inj} = 10$ Oe. In fact, when the pinning is done by slowly increasing the field from $H_{inj} = 0$ Oe (Fig. 3(a)), the peaks for TCCW (0.19 Ω) and VCCW (0.27 Ω), clearly present at H = 10 Oe, contribute to the 0.23 Ω peak at H = 30 Oe, which confirms the tendency of the AMR from the different DWs towards a single value around 0.23 Ω.

At higher fields, the simulations show that the AMR of the TCCW also tends slowly towards the AMR of a TCW pinned (3.5 mT), which might explain why at $H_{inj} = 20$ Oe, all the DWs detected have a resistance value around 0.23 Ω. Therefore, for a square notch, when the injection is done at a

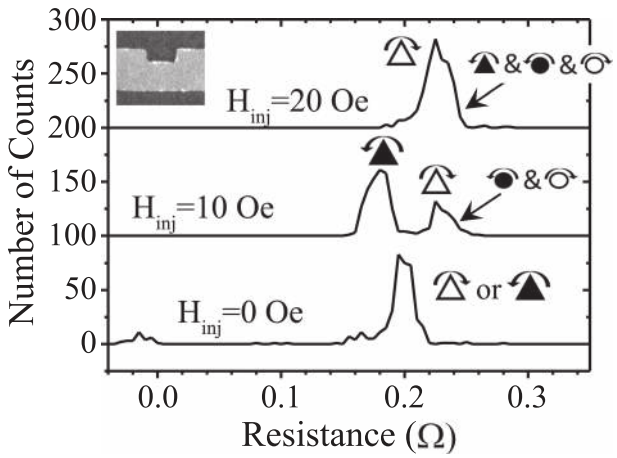

FIG. 5. Histograms for different injection fields H_{inj} in a stripe with a square notch. The corresponding micromagnetic simulations are shown in Fig. 2(b).

large field, it seems that the different types of DW might be undistinguishable.

Finally, we have studied the injection and pinning in a stripe with a circular notch. According to the simulations, a circular notch behaves in a similar fashion to a square notch. The only subtle difference is that the AMR of the TCCW has a weaker dependency with the external field. Therefore, we expected that the TCCW peak (0.19 Ω) would remain even when injecting at high fields. Indeed, that is what we observe. Fig. 6(a) shows the 0.19 Ω peak up to $H_{inj} = 20$ Oe. Noticeably, at $H_{inj} = 10$ Oe, all the AMR values for the different DWs seem to collapse to a single 0.19 Ω peak (although two humps are visible on the right hand side of the peak, indicating the presence of other types of DW). This single peak at intermediate injection fields ($H_{inj} = 10$ Oe) is unexpected and different to what is measured for other shapes of notch. Increasing the injection pulse from 1.4 V to 2.4 V does not alter the main features of the histograms (not shown). Therefore, the single peak at $H_{inj} = 10$ Oe can only be explained if the AMR values of the different types of DWs are more closed together than in other shapes of notch. This is not clear judging by the results of the simulations although, as we mentioned in Sec. II, the estimation of the AMR values is done by assuming the current flowing always in the direction of the stripe (not following the shape of the notch), so the real AMR values could be slightly different to the ones calculated. In any case, although the circular notch seems to confirm that the AMR of the different DWs evolve to set values for the different injection fields, it provides the worse discrimination of the different DWs out of all the notches.

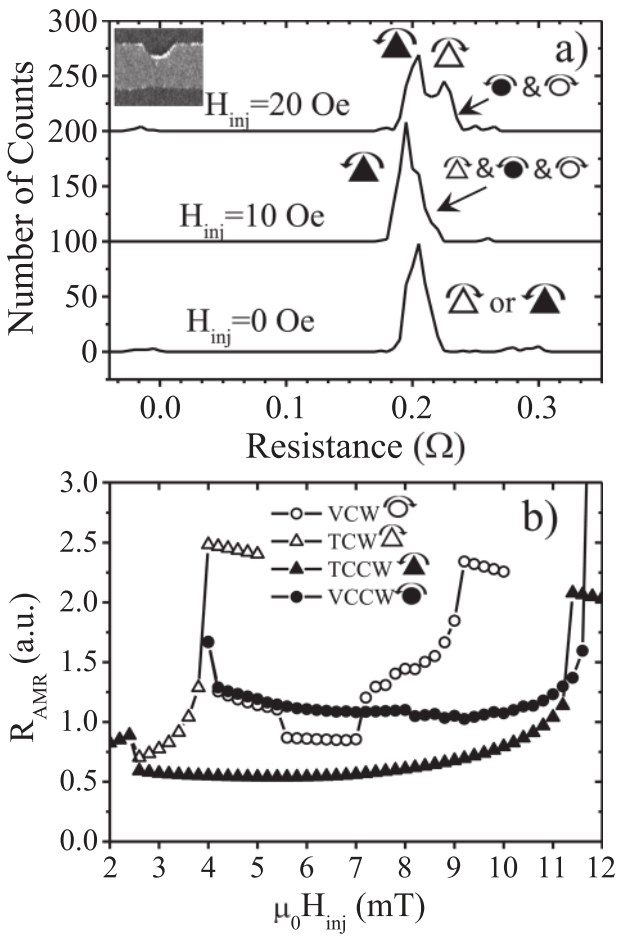

FIG. 6. (a) Histograms for different injection fields H_{inj} in a stripe with a circular notch. (b) AMR obtained from the micromagnetic simulations, for each type of DW for different stages of the pinning-depinning process.

IV. DISCUSSION AND CONCLUSIONS

The impossibility to discriminate the four types of DWs when they are injected at large fields can be caused by two factors: lack of precision of the measuring set-up or, as the simulations indicate, to the fact that the AMR of the different types of DW become quite similar to each other as the injection field increases.

Regarding the precision of our measuring set-up, we identify two main sources of error: (a) H_{inj} might not be exactly the same from one injection event to the next and (b) the background noise in the measurement of the resistance. In our experimental system, the magnetic field may oscillate ±0.1 Oe from measurement to measurement (standard deviation $\sigma = 0.1$ Oe of a histogram built out of the 400 set values of H_{inj} in any of the experiments). Also, the lock-in technique used to measure the resistance of the stripe can discriminate AMR values separated 0.005 Ω (standard deviation $\sigma = 0.005$ Ω of a histogram measuring the resistance of the stripe at saturation 400 times). Therefore, when a histogram is broad and has a standard deviation larger than $\sigma = 0.005$ Ω (in fact most of the histograms shown in this work), it represents a large and real spread of the AMR values of the pinning events, rather than a limitation of the experimental set-up.

We have seen then that the discrimination of the four different types of DW is possible for a *quasi-static* injection-pinning process, where the injection of the DW is done at a $H_{inj} = 0$, and then the external field is slowly increased until it is higher than the propagation field. The propagation field must be very small though, otherwise the larger field required to move the DW would result on a broader histogram of pinning events and the impossibility of discriminating the different DWs.

In a *dynamic* pinning process, where the DW is injected under a constant H_{inj} higher than the propagation field, our results show that the discrimination of different DWs is rather difficult. Only in very few experiments with a triangular notch, the four types of DWs could be separated by the value of their AMR. The results are presented for set values of H_{inj} (0, 10, and 20 Oe) but when the experiments were done at different values of H_{inj}, the results were equally discouraging and rarely found more than two peaks in the histograms.

Therefore, the apparent absence of some of the DWs at high or moderate H_{inj} means that, either those DWs are not traveling though the stripe for that particular H_{inj}, or that the AMR of the different DWs pinned at that H_{inj} become all quite similar to each other. With the measurements of the quasi-static pinning (see for instance, Fig. 3) and previous measurements and simulations,[18,20] we are fairly confident that all four types of DWs are travelling through the stripe once the external field is of the order of 10 Oe or larger.

Also, the estimation of the AMR for the different types of DW with the micromagnetic simulation indicates that indeed their AMR tends to get quite similar to each other as the pinning field increases, which justifies the apparent absence of some types of DW in the experimental histograms as H_{inj} increases.

Changing the shape of the notch alters slightly the pinning pattern but, in general, once the injection field is close or larger than the Walker field (about 10 Oe), the vortex DWs are difficult to separate from the transversal walls in the histograms. Therefore, as a general rule, it seems that *quasi-static* pinning combined with small propagation field, is the only reliable way of discriminating the four different types of DW in Permalloy nanostripes with dimensions that can host these four types of DWs. When the pinning is *dynamic* under a moderate or a large field, caution should be taken when associating a value of AMR to a given type of DW.

ACKNOWLEDGMENTS

This work was funded by MAT2011-28532-C03-03, MAT2011-28751-C02-01, and MAT2009-08771 from the Spanish Ministerio de Ciencia e Innovación.

[1]D. A. Allwood, G. Xiong, C. C. Faulkner, D. Atkinson, D. Petit, and R. P. Cowburn, Science **309**, 1688 (2005).
[2]S. S. P. Parkin, M. Hayashi, and L. Thomas, Science **320**, 190 (2008).
[3]L. J. Chang, P. Lin, and S. F. Lee, Appl. Phys. Lett. **101**, 242404 (2012).
[4]M. Hayashi, L. Thomas, C. Rettner, R. Moriya, X. Jiang, and S. S. P. Parkin, Phys. Rev. Lett. **97**, 207205 (2006).
[5]M. Hayashi, L. Thomas, C. Rettner, R. Moriya, and S. S. P. Parkin, Nature Phys. **3**, 21 (2007).
[6]D. Atkinson, D. S. Eastwood, and L. K. Bogart, Appl. Phys. Lett. **92**, 022510 (2008).
[7]W. Zhu, J. Liao, Z. Zhang, B. Ma, Q. Y. Jin, Y. Liu, Z. Huang, X. Hu, A. Ding, J. Wu, and Y. Xu, Appl. Phys. Lett. **101**, 082402 (2012).
[8]C. C. Faulkner, M. D. Cooke, D. A. Allwood, D. Petit, D. Atkinson, and R. P. Cowburn, J. Appl. Phys. **95**, 6717 (2004).
[9]L. K. Bogart, D. Atkinson, K. O'Shea, D. McGrouther, and S. McVitie, Phys. Rev. B **79**, 054414 (2009).
[10]U. Pi, Y. Cho, J. Bae, S. Lee, S. Seo, W. Kim, J. Moon, K. Lee, and H. Lee, Phys. Rev. B **84**, 024426 (2011).
[11]L. Bocklage, F. Stein, M. Martens, T. Matsuyama, and G. Meier, Appl. Phys. Lett. **103**, 092406 (2013).
[12]M.-Y. Im, L. Bocklage, P. Fisher, and G. Meier, Phys. Rev. Lett. **102**, 147204 (2009).
[13]J. Akerman, M. Muñoz, M. Maicas, and J. L. Prieto, Phys. Rev. B **82**, 064426 (2010).
[14]C. Wuth, L. Kolbe, and G. Meier, J. Appl. Phys. **114**, 103901 (2013).
[15]H. Fangohr, D. S. Chernyshenko, M. Franchin, T. Fischbacher, and G. Meier, Phys. Rev. B **84**, 054437 (2011).
[16]J. Torrejon, G. Malinowski, M. Pelloux, R. Weil, A. Thiaville, J. Curiale, D. Lacour, F. Montaigne, and M. Hehn, Phys. Rev. Lett. **109**, 106601 (2012).
[17]D. Ilgaz, M. Kläui, L. Heyne, O. Boulle, F. Zinser, S. Krzyk, M. Fonin, U. Rüdiger, D. Backes, and L. J. Heyderman, Appl. Phys. Lett. **93**, 132503 (2008).
[18]J. L. Prieto, M. Muñoz, and E. Martínez, Phys. Rev. B **83**, 104425 (2011).
[19]M. Hayashi, Ph.D. dissertation, Stanford University, 2006.
[20]M. Muñoz and J. L. Prieto, Nat. Commun. **2**, 562 (2011).
[21]G. S. D. Beach, C. Knutson, C. Nistor, M. Tsoi, and J. L. Erskine, Phys. Rev. Lett. **97**, 057203 (2006).
[22]L. K. Bogart, D. S. Eastwood, and D. Atkinson, J. Appl. Phys. **104**, 033904 (2008).